https://doi.org/10.5194/nhess-2021-82
Preprint. Discussion started: 29 March 2021

Natural Hazards and Earth System Sciences
Open Access
EGU
Discussions

Evaluation of the resilience of fishery ports to typhoons: a case study on Dongsha fishery port

Yachao Zhang[1], Xiaojie Zhang[1], Jufei Qiu[1], Aifeng Tao[2], Yanfen Deng[1], Jianli Zhao[1], Jianfeng Wang[1], Wentao Huang[3]
[1]East Sea Marine Environmental Investigation & Surveying Center, SOA China, Shanghai 200137, China
[2]Key Laboratory of Ministry of Education for Coastal Disaster and Protection, Hohai University, Nanjing 210098, China
[3]Shanghai East Sea Marine Engineering Survey & Design Institute, Shanghai 200137, China
Correspondence to: Jufei Qui (qjf@ecs.mnr.gov.cn)

Abstract. After standard seawalls have been built successfully, fishery ports become the structures most easily damaged during a typhoon. Assessments of the resilience of fishery ports to typhoon damage would be useful for identifying weaknesses and implementing corrective measures to protect fishing boats from a typhoon. This study describes a versatile methodology for conducting this type of quantitative assessment at fishery ports. The Dongsha fishery port in Zhejiang Province was selected as a case study to test the results derived from a high-precision Hydrodynamic Flexible Mesh model coupled with the Spectral Wave model. First, typhoon characteristics were assessed based on historical typhoons in the study area, and then, the wind, tide, storm surge, and waves were modeled and tide-surge interactions were investigated. Through comparisons of the destructive parameters from the typhoon assessment with the design and structural parameters of the fishery port, the resistance level of the Dongsha fishery port against typhoons was determined to be 12, and the main weaknesses of the port's defenses were found to be located near feature points T2, T3, T8, and T15. The results obtained demonstrate that the proposed methodology can be used to acquire valuable information on the resilience of fishery ports to typhoons.

1 Introduction

As one of the countries with the largest fishery resources around the world, China ranks first in the world in terms of the output of aquatic products, number of fishing boats, and number of fisheries employees (NDRC and MARA, 2018). However, as China lies on the west coast of the Pacific Ocean, its coastal areas are susceptible to various marine disasters, especially typhoons and storm surges (Ministry of Natural Resources of the People's Republic of China, 2019). Within China, Zhejiang Province near the East China Sea is well-known for fishing. The total marine fishery production output here was ranked first nationally at 3,200,000 t. Coastal areas within Zhejiang, especially the city of Wenzhou, are vulnerable to typhoon-related damage (Du et al., 2020; Shi et al., 2020b). Almost every year, more than one typhoon strikes the coast of Zhejiang Province, and these typhoons frequently cause damage to the breakwater structures, wharfs, and fishing boats. According to the Zhejiang Marine Disaster Bulletin (2019), a total of 2064 fishing boats were damaged by typhoons, and the direct economic losses due to typhoons amounted to 87.25 hundred million yuan (Department of Natural Resources of Zhejiang Province, 2019). Since record keeping began, the largest storm surge event near the Dongsha fishery port occurred in 1997 (210 cm at the Kanmen tide gauge station). Significant fluctuations in the sea level are caused by the strong winds in the low-pressure storm systems that cross over the Dongsha fishery port. As storms pass over the sea, the conditions create storm surges. Low atmospheric pressure and winds cause an increase in water levels at nearby coastal areas, which often leads to flooding (Wang et al., 2017). After standard seawalls are successfully built, disaster prevention and mitigation efforts at fishery ports become particularly important. Knowledge of the degree of resilience of fishery ports to typhoons would be of great benefit to disaster prevention plans and coordination of mitigation activities within a region.

Most research on fishery ports has focused on the biology and ecology of a port and its geomorphic stability. However, the ability of fishery ports to resist the damage caused by typhoons has not received much research attention yet. Notably,

https://doi.org/10.5194/nhess-2021-82
Preprint. Discussion started: 29 March 2021

Natural Hazards and Earth System Sciences Discussions
Open Access

Premwadee et al. (2006) studied the trends in marine fish catches at the Pattani fishery port, and Kawaguchi et al. (1995) presented construction recommendations for an offshore fishery port to prevent coastal erosion following hydraulic model tests and numerical simulations of wave induced currents near the port. Additionally, there have been numerous studies about the risks of hurricanes or typhoons at home and abroad. In America, the National Weather Service storm surge model, named SLOSH (Sea, Lake, and Overland Surge from Hurricanes), has been used to delineate coastal areas susceptible to hurricane storm surge flooding (Glahn et al., 2009). A computer simulation of super typhoon Haiyanin with the resulting wave heights and storm surge levels was made using the MIKE21 model in Tacloban city (Prelligera et al., 2014). Li et al. (2020) examined the dependence of typhoon-induced storm surge and wave setup effects on the typhoon intensity and size. MIKE21 was also used to evaluate the overtopping risk of seawalls and levees from the combined effects of the storm tide, sea level rise, and land subsidence in Shanghai (Wang et al., 2011). A methodology for storm surge risk assessments in coastal counties was established following research in Jinshan District, Shanghai city (Shi et al., 2020a).

Estimating the resilience of fishery ports to typhoons is a difficult task. In particular, because each fishery port is different in terms of its geographical location, topography, anchoring water, and shape, we cannot carry out one assessment under the same typhoon conditions or even for completely different typhoons. Additionally, the storm surge can be influenced significantly by the landfall location of a typhoon with the same pressure (Sun et al., 2015). Abeshima et al. (2017) clarified the mechanism of port disturbance generation at the Kumaishi fishery port and concluded that the quantitative indicator $H_{1/3}$ (over 2.0 m) can be introduced as a decision indicator for evacuations by observational statistics. Some exploratory work has been conducted in China on fishery ports' resistance to damage caused by typhoons. Notably, one study used an analytical hierarchy process for indexes of wind and wave features, the number of sheltering boats, anchoring methods, emergency measures, and the local management system to assess the relative preparedness of fishery ports in Xiamen against typhoons (Dongshui and Qionglin, 2019). Based on the nested model of Delft3D, the fishery ports were first evaluated in terms of the following three aspects: the level of shoreline facilities, anchorage areas, and breakwaters to lessen typhoon impacts. However, the maximum observed frequency of the wind direction was roughly regarded as the typhoon pathway, which was the key factor in that study. Importantly, the interaction of the tide and surge was not taken into account.

This study describes a systematic and quantitative method for assessing the resilience of fishery ports to typhoons. The method can be used to conduct comparisons among different fishery ports, and the proposed method also relies on basic data for the three aspects described above. Additionally, the typhoon resistance capability of a fishery port is indicated by the sustainable maximum wind scale of the port. Meanwhile, typhoon pathways and tide-surge interactions, the key factors of the assessment, are studied in detail. After deriving a quantitative value for the resistance level of a fishery port against typhoons, effective countermeasures for typhoons can be proposed, and such data should also be useful for making judgments as to the need for evacuations by administrators.

2 Materials and methods

2.1 Study area

The Dongsha fishery port is located on the east side of Dongtou Island (121°10′–121°11′E and 27°50′–27°51′N) in the city of Wenzhou, China (Fig. 1). It is C-shaped and surrounded on three sides by mountains, which makes it a natural sheltered harbor for fishing boats. Presently, it is the best sheltered harbor in Wenzhou. The length of the fishery port coast is 5.17 km, and there is a 0.35 km long breakwater, which was built at the entrance of the fishery port. The water area of the port is approximately 750,000 m^2 with a depth of 3–9 m.

https://doi.org/10.5194/nhess-2021-82
Preprint. Discussion started: 29 March 2021

Natural Hazards and Earth System Sciences
Open Access
Discussions

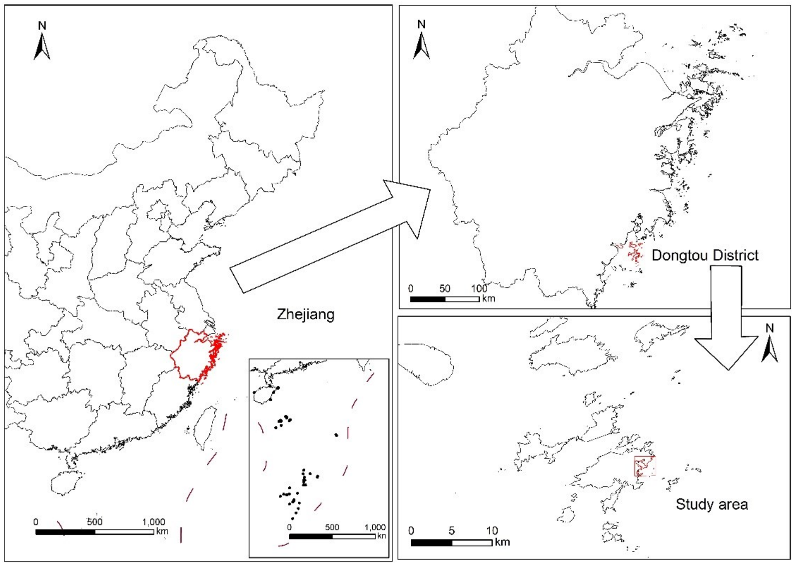

Figure 1. Study area in Dongsha, Wenzhou, China.

2.2 Data

To model a specific area of a vulnerable fishery port, accurate topographic, meteorological, and other types of basic data are required. Here, multisource data were classified into four types (Table 1) and were used to run and validate the Hydrodynamic Flexible Mesh (HD FM) model coupled with the Spectral Wave (SW) model for the Dongsha fishery port. The topographic data, which were at the same datum plane, were collected to construct the numerical model, and the meteorological data and hydrologic data were used as dynamic data and validation data for the numerical model. The design and structural parameters of the Dongsha fishery port were compared with the numerical simulation results, and then, these results were used to judge the resistance of the port.

Table 1. Multisource data used to perform and validate the model.

Data type	Element	Time series	Description	Source
Meteorological data	Wind	1961–2015	Wind velocity and direction	Wenzhou Marine Environmental Monitoring Center
	Historical typhoon records	1949–2018	Time, location, and intensity of each typhoon track point	China Meteorological Administration
Hydrological data	Tide	2014.10	Hourly tidal level	Wenzhou Marine Environmental Monitoring Center
	Storm surge	1997–2015	\	Wenzhou Marine Environmental Monitoring Center
	Current	2014.10	Hourly flow velocity and direction	Actual measurement
	Wave	1997–2015	Significant wave height	Wenzhou Marine Environmental Monitoring Center
Topographical data	Topography	2016.1	Depth of fishery port and chart	Actual measurement and chart
	Bottom characteristics	2015.03	Bottom characteristics of fishery port	Actual measurement
Data about fishery port facilities	Shoreline	\	Elevation of shoreline	Actual measurement
	Seawall	\	Elevation of seawall	Actual measurement
	Fishing-boat	\	Length, width and draught	Actual measurement
	Anchor	\	Weight and length	Actual measurement

2.3 Methods

In this study, a framework (Fig. 2) is proposed for evaluating the resilience of fishery ports to typhoon related damage. The framework is composed of the following five parts: typhoon building, model configuration and verification, hazard simulation,

https://doi.org/10.5194/nhess-2021-82
Preprint. Discussion started: 29 March 2021

Natural Hazards and Earth System Sciences
Open Access
Discussions

individual assessment, and comprehensive assessment.

For typhoon building, for the convenience of reading, there are some terms that need to be explained first. The *influential typhoons* refer to historical typhoons that have had an impact on the study area within a certain distance. The *typical typhoons* are typhoon categories classified from the influential typhoons by certain rules. The *alternative assessment typhoons* refer to alternative typhoon prototypes that are representative in each typical typhoon category. The final *assessment typhoon* is the typhoon with the maximum destructive parameters among the alternative assessment typhoons.

Using MIKE21 software, the current, storm surge, and waves under various typhoon scenarios were simulated. These scenarios provided the information required for the assessment and were chosen so that the data would cover future typhoon events anticipated to have significant impacts on the Dongsha fishery port. The wind data and current data were used to calculate the stresses on fishing boats, which were compared with the holding power of anchors. The resilience of the anchorage to typhoon damage was represented by the minimum typhoon intensity when the force from the wind and currents was larger than the holding power of the anchor. In a similar manner, the resilience of the shoreline facilities to typhoon damage was represented by the minimum typhoon intensity when the water level of storm surge adding to 1/2 the significant wave height was higher than the coastline elevation. Similarly, the resilience of the seawall to typhoon damage was represented by the minimum typhoon intensity when the significant wave height or the sheltered area of the typhoon was higher than the design wave of the seawall.

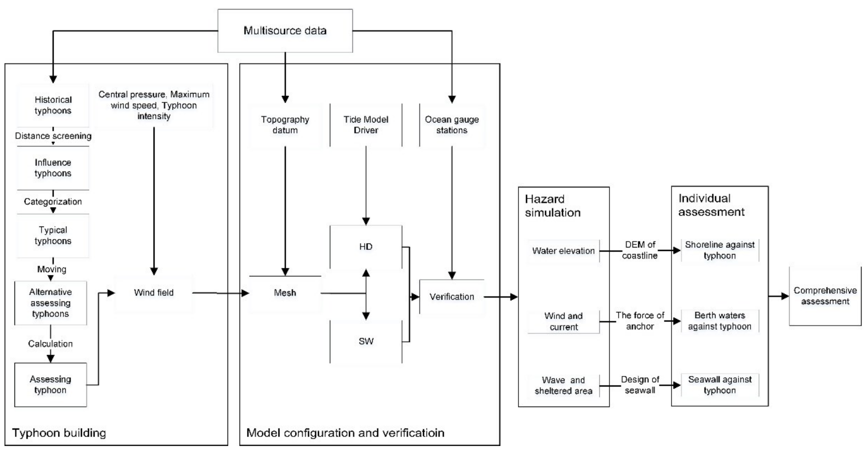

Figure 2. Framework for assessing the resilience of fishery ports to typhoon damage.

2.3.1 Numerical model configuration

The 2D shallow water model has been shown to reproduce storm surges well (Bertin et al., 2012). Notably, MIKE21 was used successfully for the simulation of tidal waves during a storm surge in the north part of Liaodong Bay (Kong, 2014). In this study, the MIKE21 model was used to construct the hydrodynamic module, storm surge, and typhoon waves. The model was based on a flexible mesh approach. Simulations were made by using the SW model coupled with the HD FM model of the software. The SW model solved for the wave action density, data which grew with the wind and dissipated owing to white capping, surf breaking, bottom friction, and nonlinear interactions between spectral components in deep and shallow waters. MIKE21 FM uses the finite volume method to solve the Navier–Stokes equations. Unstructured meshes were used in the model, along with atmospheric pressure and wind. Detailed information for MIKE21 can be found in the scientific documentation and user guide for the model (DHI, 2012).

The inset of Fig. 3 shows the computational domain and the mesh grid. It covered a large area that ranged from 106° to 135°E and 12° to 41°N; a large area was used to properly reproduce storm surges and waves generated at a greater distance from the Dongsha fishery port. The grid used was fine near the area of interest and decreased in resolution in the deepwater

https://doi.org/10.5194/nhess-2021-82
Preprint. Discussion started: 29 March 2021

Natural Hazards and Earth System Sciences
Open Access
EGU
Discussions

area where minute details were not as important. There were 67,549 grid cells and 35,899 nodes, which became denser closer to the Dongsha fishery port. The minimum resolution of the grid size was 20 m, which could embody the seawall, wharf, and other structures. The bathymetry data were obtained from several charts from the Maritime Safety Administration of the People's Republic of China and actual measurements, which were unified at the same datum plane of the 1985 national height datum.

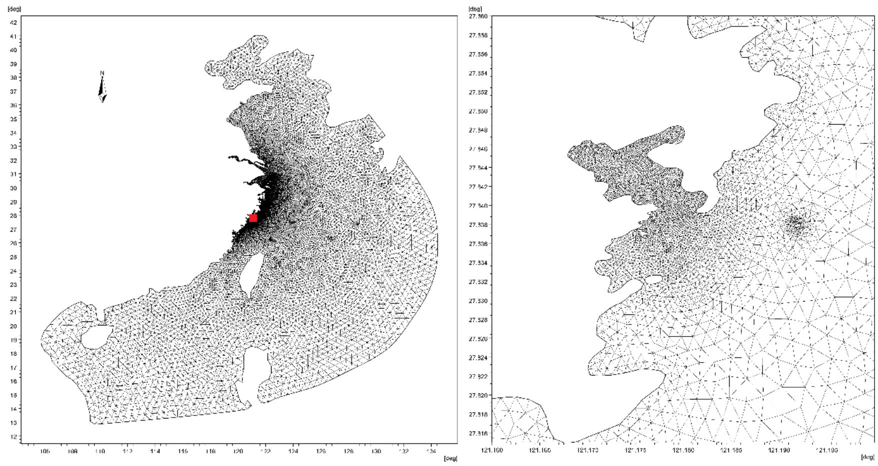

Figure 3. Mesh grid in the numerical model and grid of the interest area.

2.3.2 Numerical model verification

The typhoons of 9711, 0509, 0713, 0716, and 1509 were selected when the observed values were the maximum or the typhoon caused relatively extensive damage. The numbers published by the China Meteorological Administration are indicative of the year and order of typhoons that have impacted China, for example, 9711 means the 11th typhoon that occurred during 1997. There were some ocean gauge stations near the Dongsha fishery port, and each station observed different oceanographic elements. The storm surge model was validated with the data from the Kanmen and Wenzhou tide gauge stations. The wave model was validated with the data from the Nanji and Wenzhou wave gauge stations. The whole hourly storm surge was processed by simulations under various scenarios with and without a typhoon to extract the tide. To validate the surge, observed and modeled water levels were compared. Figure 4 and 5 shows that there was a good correlation between the data from the tide gauge stations and the model results, both in terms of the phase and amplitude. Because the maximum data were more important during the assessment, Tables 2 and 3 respectively show the relative error of the maximum storm surge and waves. The relative error of the maximum storm surge was 21.89 %, and that of the waves was 12 %. Modeling with good results very similar to the observed data was very difficult to achieve, as the wind, rain, current, and wave interactions were complex during a typhoon. However, the preliminary results showed that it was possible to forecast the effects of storm surges and waves by several days in advance.

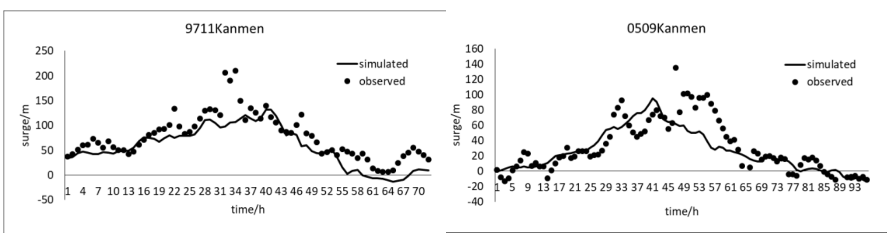

https://doi.org/10.5194/nhess-2021-82
Preprint. Discussion started: 29 March 2021

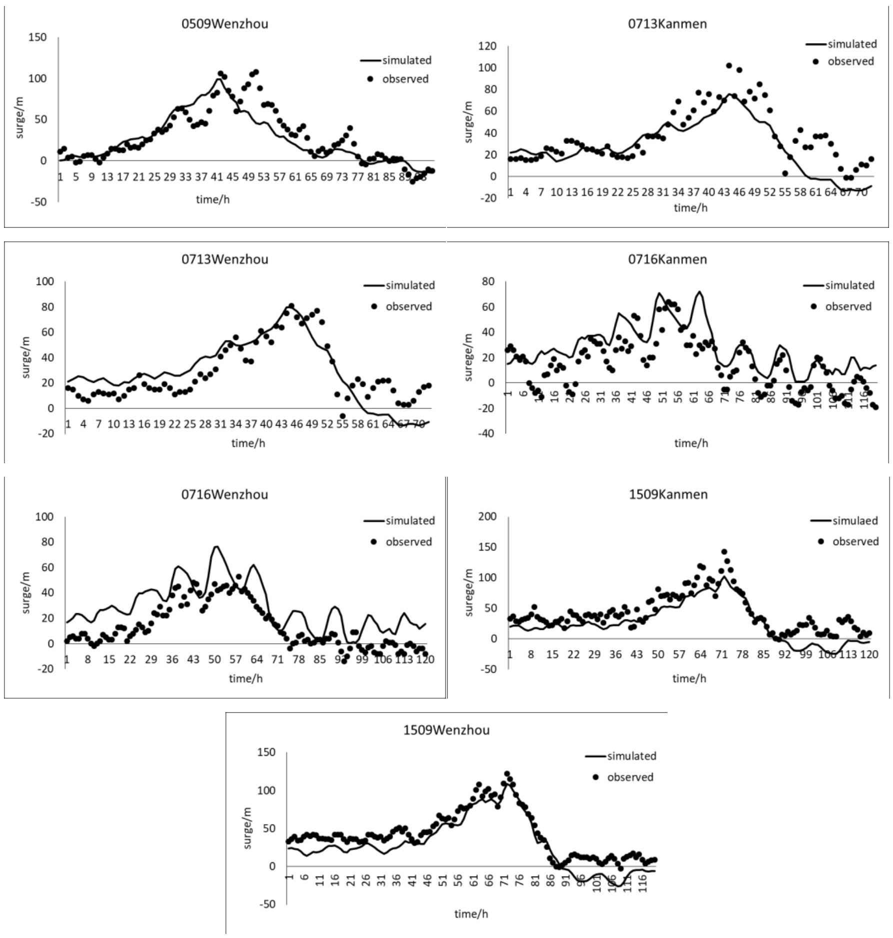

Figure 4. Comparison of the storm surge at Nanji and Wenzhou stations.

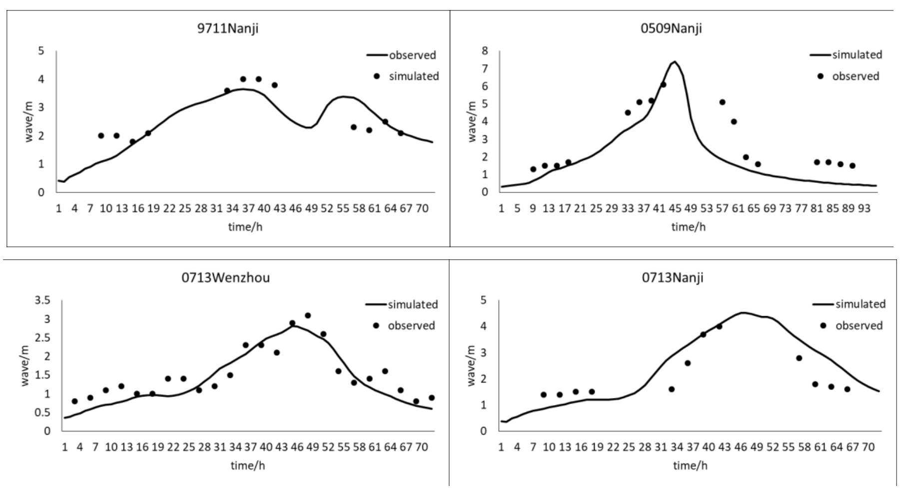

https://doi.org/10.5194/nhess-2021-82
Preprint. Discussion started: 29 March 2021

Natural Hazards and Earth System Sciences
Discussions

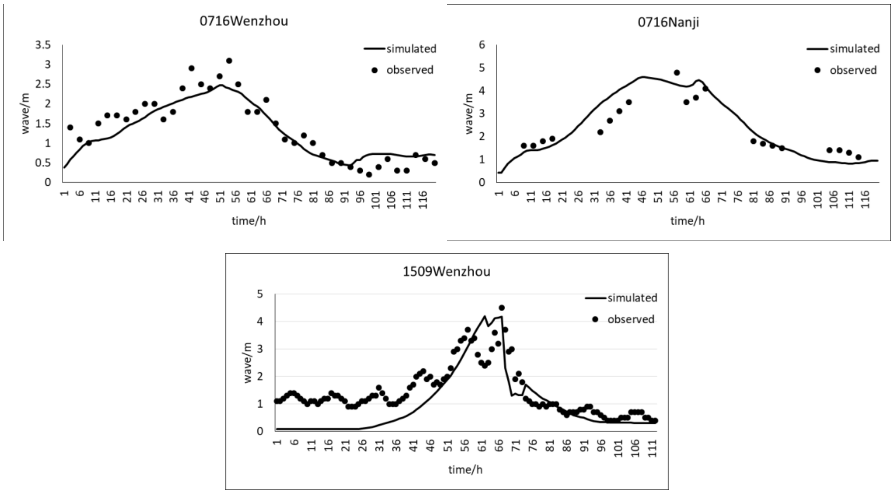

Figure 5. Comparison of the waves at Nanji and Wenzhou stations.

Table 2. Relative error of the storm surge.

Typhoon	Station	Storm surge		Relative error
		Observed (m)	Modeled (m)	
9711	Kanmen	2.10	1.90	9.5 %
0509	Kanmen	1.35	0.95	29.6 %
	Wenzhou	1.08	0.99	8.3 %
0713	Kanmen	1.02	0.76	25.5 %
	Wenzhou	0.59	0.42	28.8 %
0716	Kanmen	0.64	0.72	12.5 %
	Wenzhou	0.53	0.76	43.4 %
1509	Kanmen	1.43	1.02	28.7 %
	Wenzhou	1.22	1.09	10.7 %

Table 3. Relative error of the waves.

Typhoon	Station	Wave		Relative error
		Observed (m)	Modeled (m)	
9711	Nanji	4	3.6	10 %
0509	Nanji	6.1	7.4	21 %
0713	Nanji	3.1	2.9	6 %
	Wenzhou	4	4.5	13 %
0716	Nanji	3.1	2.4	23 %
	Wenzhou	4.8	4.6	4 %
1509	Wenzhou	4.5	4.2	7 %

2.3.3 Typhoon prototype selection/ storm track

Influence typhoons were chosen by a method of distance screening from the history of typhoons, which amounted to 1841 typhoons in total for China during the period 1949–2017. The method of distance screening involved drawing a circle with the fishery port at the center and a radius of 40 km. This radius was set because the geometric mean radius of maximum wind is

https://doi.org/10.5194/nhess-2021-82
Preprint. Discussion started: 29 March 2021

Natural Hazards and Earth System Sciences
Discussions

47.5 km in the Atlantic and eastern Pacific (Willoughby and Rahn, 2004) and concentrated at 40 km in the western North Pacific (Yang et al., 2017). The influential typhoons were classified in order to determine typical typhoon conditions. Assessment of the typhoons was carried out with the maximum risk for alternative assessment typhoons according to the results of simulations.

First, 1841 historical typhoon pathways were collected from the tropical cyclone information center of the China Meteorological Administration, and these typhoons all occurred from 1949 to 2017. Next 123 influential typhoons were chosen by the method of distance screening from the abovementioned historical typhoon pathways (Fig. 6). Because the influential typhoons occurred in all directions, the influential typhoons were categorized into four typical typhoon patterns according to their pathways as shown in Fig. 7. At the same time, by considering the opening direction of the Dongsha fishery port where the seawall gap faces toward the southeast, the typhoon pathway toward the northwest was selected as the fifth typical typhoon pattern. Then, five representatives were selected from each typical typhoon pattern. Next, five representatives were moved to a radius of 40 km around the Dongsha fishery port, and these represented the alternative assessment typhoons (Fig. 8 and Table 4).

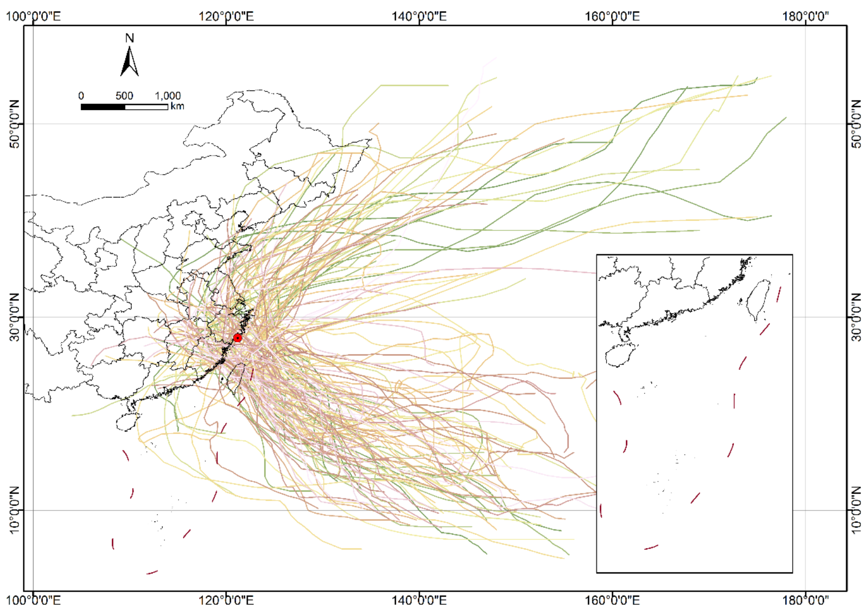

Figure 6. Pathways of influential typhoons.

https://doi.org/10.5194/nhess-2021-82
Preprint. Discussion started: 29 March 2021

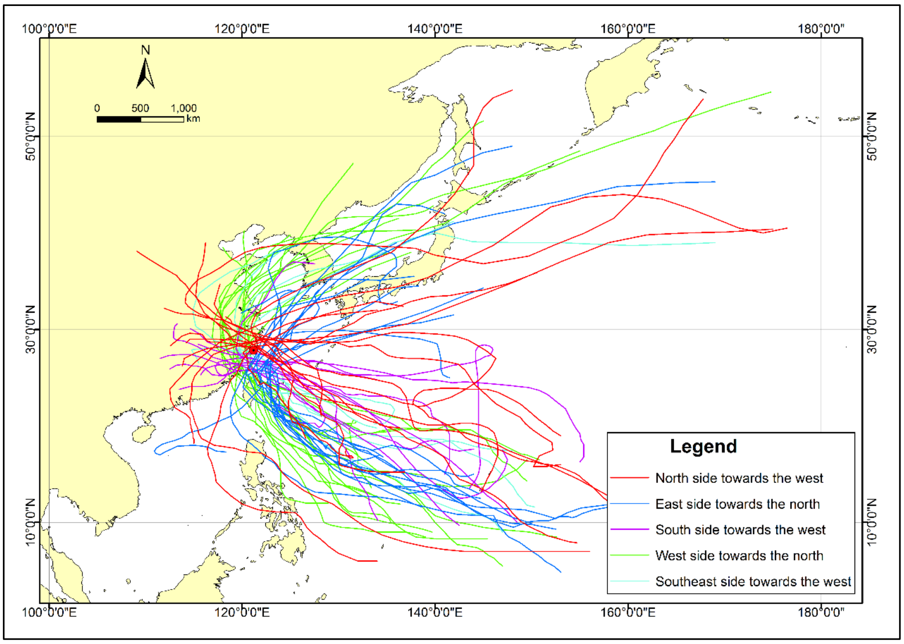

Figure 7. Pathways of typical typhoons.

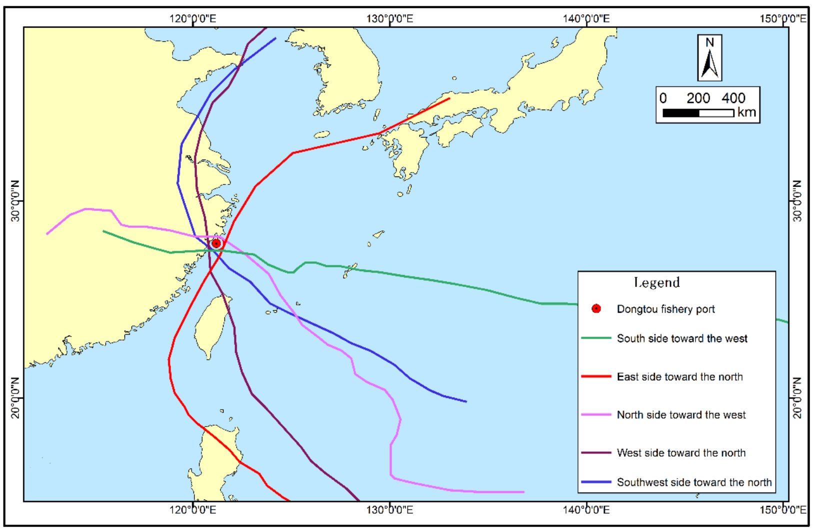

Figure 8. Pathways of alternative assessment typhoons.

Table 4. Pathways of alternative assessment typhoons.

	Alternative assessment typhoons	Typhoon prototype number	Typhoon prototype name
1	East side toward the north	/	Virginia
2	West side toward the north	8707	Alex
3	South side toward the west	0216	Sinlaku
4	North side toward the west	0414	Rananim

https://doi.org/10.5194/nhess-2021-82
Preprint. Discussion started: 29 March 2021

Natural Hazards and Earth System Sciences
Discussions

5	Southeast side toward the west	0713	Wipha

Five scenarios of different alternative assessment pathways under a level 17 typhoon were calculated, including the storm surge and typhoon waves. Seven feature points, as shown in Fig. 9, were extracted from the results to reflect the area of the seawall (B1), entrance (B2), anchorage water (B3, B4), wharf (B5, B6), and Dawangdian Bay (B7). The south side toward the west scenario was selected as the final assessment typhoon pathway (Fig. 10), during which the storm surge and waves were at the maximum values at the feature point (Table 5).

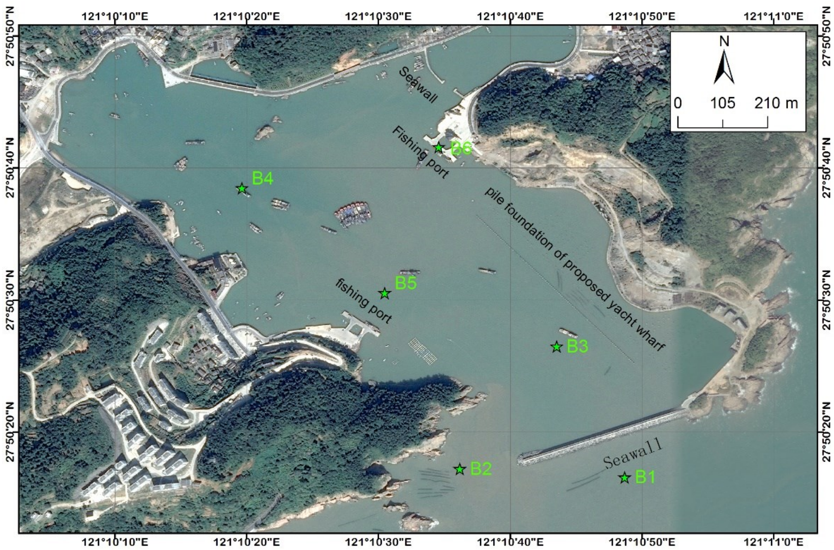

Figure 9. Feature points of the five alternative assessment typhoon scenarios (from © Google Earth).

Table 5. Results for the five typhoon pathways.

Feature point	East side toward the north		West side toward the north		South side toward the west		North side toward the west		Southeast side toward the west	
	Surge	Wave	Surge	Wave	Surge	Wave	Surge	Wave	Surge	Wave
B1	0.72	3.49	0.57	2.74	2.03	3.61	1.70	1.57	0.80	3.14
B2	0.72	3.12	0.57	2.55	2.04	3.34	1.71	1.57	0.81	2.76
B3	0.72	0.31	0.57	0.22	2.03	0.28	1.71	0.10	0.81	0.27
B4	0.73	0.21	0.58	0.16	2.06	0.21	1.74	0.08	0.82	0.15
B5	0.73	0.11	0.57	0.09	2.05	0.12	1.73	0.04	0.82	0.08
B6	0.73	0.35	0.57	0.26	2.04	0.34	1.73	0.12	0.81	0.27
B7	0.73	0.14	0.57	0.11	2.04	0.14	1.73	0.05	0.81	0.11
Mean	0.73	1.10	0.57	0.88	2.04	1.15	1.72	0.50	0.81	0.97
Maximum	0.73	3.49	0.58	2.74	2.06	3.61	1.74	1.57	0.82	3.14

https://doi.org/10.5194/nhess-2021-82
Preprint. Discussion started: 29 March 2021

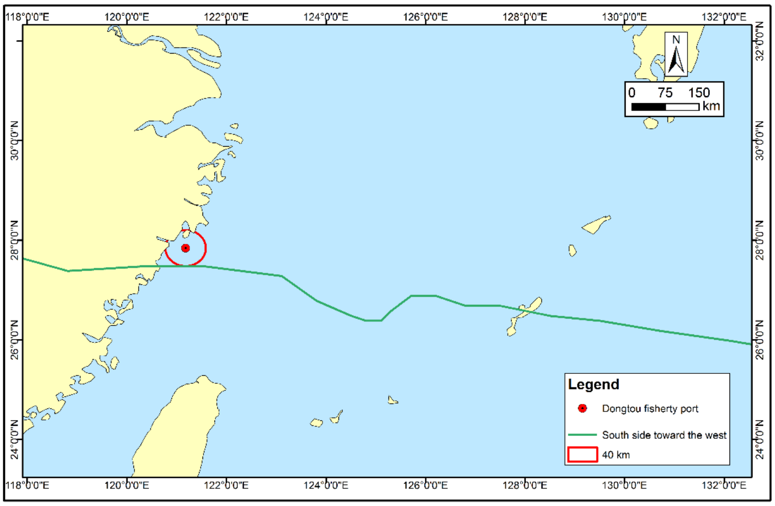

Figure 10. Pathway of the assessment typhoon.

In this study, the main approaches used for the typhoon wind field modeling were described by the Fujita Model, which has been employed in this area (Huang, 2017; Fujita, 1952).

2.3.4 Parameter setting

The tide of the open boundary was determined by using the tide obtained from the Tide Model Driver (TMD) package with its harmonic components (M2, S2, N2, K2, K1, O1, P1, Q1, and M4). The resulting forcing had a time step of 1 h. The input parameters for the wind model were the radius of maximum winds, traveling speed, and pressure difference between the storm's central pressure and the ambient (or peripheral) pressure. The radius of maximum winds was estimated from available observations by using a previously published empirical formula (Eq. (14). Zhu and Huang, 2002):

$$R = R_k - 0.4\times\left(P_0 - 900\right) + 0.01\times\left(P_0 - 900\right)^2 \quad (1)$$

where R_k is the empirical parameter (usually a value of 40 km was used), R is the radius of maximum winds, and P_0 is the central pressure.

The traveling speed for the forward velocity of the storm was obtained from the observed value of the prototype typhoon, for which data were collected from the China Meteorological Administration. The pressure difference of the typhoon was derived from the wind information provided in the typhoon history. According to experience and norms (China Meteorological Administration, 2006), 10 different values for the central pressure were used, namely, 995, 991, 985, 975, 965, 955, 945, 935, 925, and 915 (Table 6).

Table 6. Wind and pressure parameters of simulated typhoons.

Typhoon level	8	9	10	11	12	13	14	15	16	17
Maximum wind speed (m s^{-1})	20	24	27	31	35	40	44	49	53	57
Central pressure (hPa)	995	991	985	975	965	955	945	935	925	915

2.3.5 Assessment

The forces exerted on fishing boats from wind were divided into lateral and vertical directions as follows:

$$F_{xw} = 73.6\times10^{-5} A_{xw} V_x^2 \zeta_1 \zeta_2 \quad (2)$$

$$F_{yw} = 49.0\times10^{-5} A_{yw} V_y^2 \zeta_1 \zeta_2 \quad (3)$$

where F_{xw} and F_{yw} are the component forces from wind in the lateral and vertical directions (kN), respectively; A_{xw} and A_{yw} are the above water force area in the lateral and vertical directions (m^2), respectively; V_x and V_y are the wind speed in the lateral and vertical directions (m s^{-1}), respectively; ζ_1 is a nonuniform coefficient that was set to the recommended value of 1 in this study; and ζ_2 is the altitude correction factor that was set to the recommend value of 1 in this study (Ministry of Transport of the People's Republic of China, 2006).

The forces exerted on fishing boats from currents were calculated by the following formulas:

$$F_{xsc} = C_{xsc} \frac{\rho}{2} V_2 B' \quad (4)$$

$$F_{ysc} = C_{ysc} \frac{\rho}{2} V_2 B' \quad (5)$$

where F_{xsc} and F_{ysc} are the component forces from currents in the lateral and vertical directions (kN), respectively; C_{xw} and C_{yw} are the coefficients of the fore and aft, which were obtained from a look-up table (Ministry of Transport of the People's Republic of China, 2006) as 0.09 and 0.04, respectively; V is the current speed (m s^{-1}); ρ is the water density (kg m^{-3}); and B' is the underwater area of the lateral direction (m^2).

The force exerted on the ships was the resultant force of the wind and current:

$$\sum F = \sqrt{\left(\sum F_x\right)^2 + \left(\sum F_y\right)^2} \quad (6)$$

The anchor holding power of fishing boats was calculated by the following formula:

$$P = P_a + P_c = \lambda_a W_a + \lambda_c W_c l \quad (7)$$

where P is the resultant force of anchor holding (kN); P_a is the force of anchor holding (kN); P_c is the force of anchor chain holding (kN); λ_a is the coefficient of the anchor, which was set to 3.5 in accordance with the clayey silt bottom material; λ_c is the coefficient of the anchor chain, which was set to 0.6 in accordance with the clayey silt bottom material; W_a is the anchor weight, which was set to 0.15 t, 0.5 t, and 0.7 t for large, medium, and small types of fishing boats; W_c is the anchor chain weight per meter; and l is the length of the anchor chain underground. The resultant force of the fore and aft was 1.3 times the resultant force.

3 Results

The water level is presumed to be a superposition of the tide and surge. The impacts of typhoon parameters on the storm were studied (Wang et al., 2020). Storm surges are known to have some potential interactions with tides (Flather, 2001). Idier et al. (2012) concluded that the instantaneous tide–surge interaction is non-negligible in the eastern half of the English Channel, where it reaches values of 74 cm in the Dover Strait. From an operational perspective, an understanding of this interaction is of value in order to choose relevant strategies in the risk analysis. Thus, to better assess the resistance level of the fishery port against typhoon damage, tide–surge interactions were investigated.

The coupling processes of storm surges and tides were simulated in the following way. The surges were computed by gradually adding 2 h tide interactions under the level 17 typhoon. Considering the tide period in this area, there were seven scenarios. "ST-2" represented 2 h after the "ST" scenarios, and "ST+2" represented 2 h before the "ST" scenarios. In this study, as shown in Table 7, the maximum storm surge occurred during the "ST-6" scenarios, that is, most of the largest practical storm surges occurred around low tide, which is similar to results of the other study (Idier et al., 2012). Then, "ST-6" scenarios as tide–surge interaction conditions were used for further simulation.

Table 7. Storm surge for different scenarios under a level 17 typhoon (cm).

Scenario	Feature point						
	B1	B2	B3	B4	B5	B6	B7
ST-6	253	255	255	260	258	257	257
ST-4	242	244	244	248	246	246	246
ST-2	222	223	222	225	225	224	224
ST	203	204	203	206	205	204	204
ST+2	207	208	208	211	210	209	209
ST+4	218	220	219	223	222	221	221
ST+6	229	231	231	235	233	233	233

Two types of runs were implemented with the HD model, namely, one with the forcing (tide, wind, atmospheric pressure) and the other with the tide only. Based on historical storms and in collaboration with constructive typhoon characteristics, a suit of typhoon scenarios under level 8–17 typhoons were created for surge and wave modeling using HD and SW. These scenarios provided the information required for the assessment and were chosen so that the data would cover future typhoon events anticipated to have significant impacts on the Dongsha fishery port.

Next the results will be analyzed considering the following three aspects: seawall, berth waters, and shoreline.

3.1 Seawall

The design and construction data for the seawall shows that the design wave elements $H_{1/3}$ of a 50-year return period is 6.5 m at the seawall head, and the $H_{1/3}$ was 6.7 m at the seawall toe. The data extracted from typhoon scenario calculations were compared with the design wave elements (Tables 8 and 9). The design wave elements are smaller than the calculated elements at both the seawall head and seawall toe under a level 13 typhoon. Additionally, to resist a typhoon, the design wave elements should be larger than the calculated elements. Thus, from the design wave point, the resistance level of the Dongsha fishing against typhoon damage is 12.

Table 8. H_s at seawall feature points under different typhoon levels.

Typhoon level	H_s at seawall head (m)	H_s at seawall toe (m)
8	3.5	3.6
9	4.2	4.2
10	5.3	5.1
11	6.2	6.1
12	6.4	6.3
13	7.1	7.0
14	7.3	7.3
15	7.7	7.8
16	8.3	8.2
17	8.3	8.5
Design wave elements	6.5	6.7

According to the design data, the sheltered areas for large, medium, and small types of fishing boats are 70,000 m^2, 280,000 m^2, and 180,000 m^2, respectively. Anchoring wave conditions of large, medium, and small types of fishing boats are 1.2 m, 1.0 m, and 0.5 m, respectively. A distribution map of the wave amplification that propagated into the port is shown in Fig. 11.

https://doi.org/10.5194/nhess-2021-82
Preprint. Discussion started: 29 March 2021

Because it is shielded by Dongtou Island, inrushing waves at the fishery port are small. The sheltered areas of level 8–17 typhoon scenarios are presented in Table 9. The areas where $H_{1/3}$ is smaller than 0.5 m, 1.0 m, and 1.2 m are compared between the design and simulation. For instance, the design area where $H_{1/3}$ < 0.5 m is 18 × 10^4 m^2, which is much smaller than the simulated sheltered area 65.1 × 10^4 m^2 under the level 8 typhoon. Under the same typhoon level, the design area where $H_{1/3}$ < 1.0 m is (18+28) × 10^4 m^2, which is still smaller than the simulated sheltered area (65.1+3.1) × 10^4 m^2. Similarly, the design area where $H_{1/3}$ < 1.2 m is (18+28+7) × 10^4 m^2, which is also smaller than the simulated sheltered area (65.1+3.1+0.2) × 10^4 m^2 under the level 8 typhoon. Thus, we could conclude that the Dongsha fishery port can resist the level 8 typhoon from the aspect of the sheltered area. In a similar manner, the comparisons were carried out at the remaining typhoon levels. The results showed that the maximum resistance level of the Dongsha fishery port against typhoon damage is 16.

According to the principle of high not low, the resistance level of Dongsha fishery port against typhoon damage is 12.

Table 9. Sheltered area under different typhoon levels.

$H_{1/3}$ (m)	Design area ($\times10^4$ m^2)	Sheltered area under different typhoon levels ($\times10^4$ m^2)									
		8	9	10	11	12	13	14	15	16	17
$H_{1/3}$ < 0.5	18	65.1	62.2	53.5	48.3	44.9	41.6	37.7	34.1	35.1	0.0
0.5 < $H_{1/3}$ < 1.0	28	3.1	5.6	13.4	17.3	19.0	20.2	21.4	18.7	19.4	49.2
1.0 < $H_{1/3}$ < 1.2	7	0.2	0.3	0.6	1.4	2.3	3.3	4.5	7.2	6.8	5.3

https://doi.org/10.5194/nhess-2021-82
Preprint. Discussion started: 29 March 2021

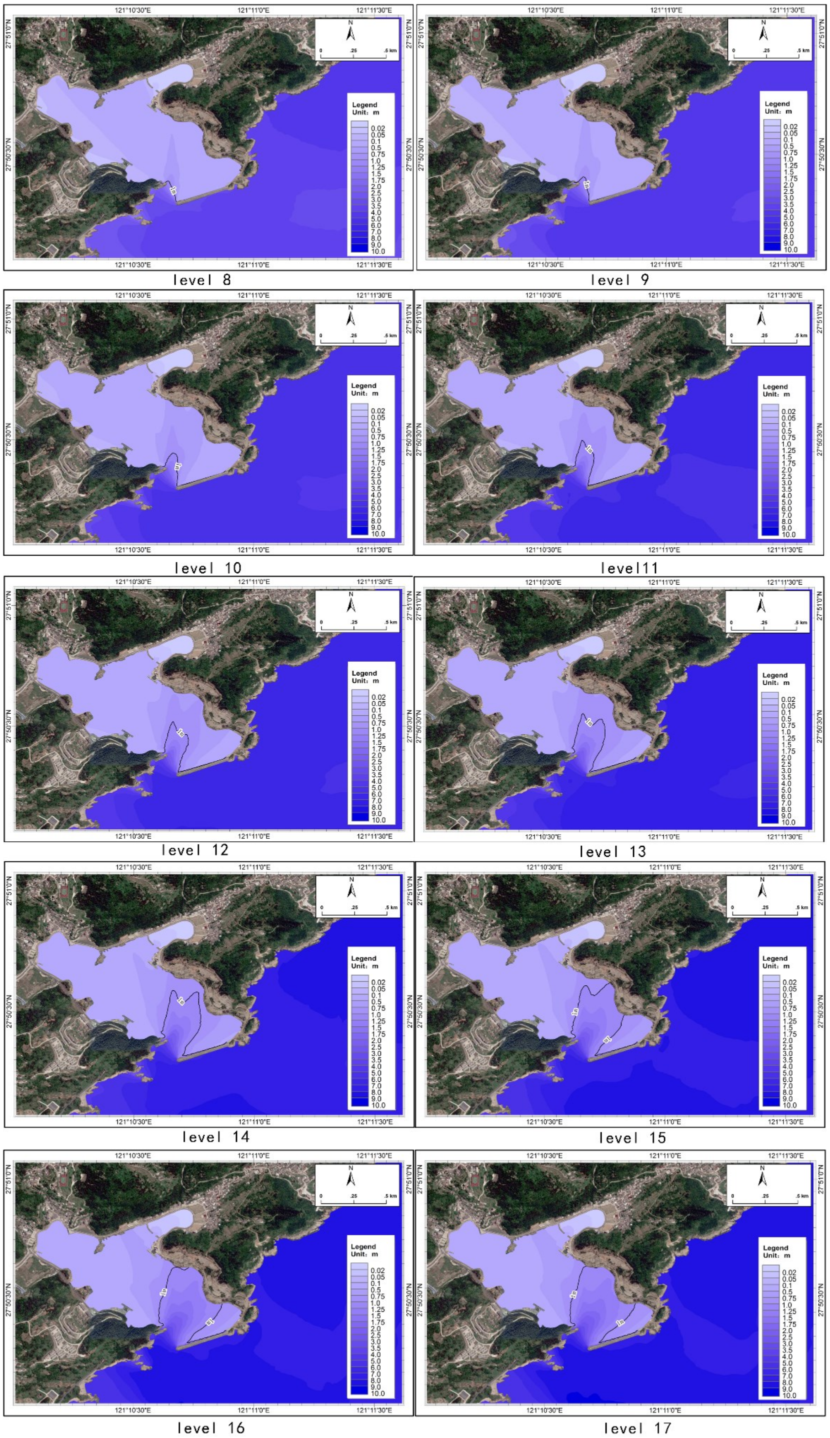

Figure 11. Distribution maps of the waves under level 8–17 typhoons (from © Google Earth).

3.2 Berth waters

A total of 23 feature points were selected for fishing boats anchored in water in accordance with information from the fishery

https://doi.org/10.5194/nhess-2021-82
Preprint. Discussion started: 29 March 2021

port's administration department (Fig. 12). In Fig. 12, the rectangles represent berth waters and the feature points are at the centers of the rectangles. Considering the long period force on fishing boats, the data for the wind and currents at those points were extracted from a suit of typhoon scenarios under level 8–17 typhoons (Table 10).

Table 10. Force from wind and currents under different typhoon levels (kN).

Feature point	Force under different typhoon levels									
	8	9	10	11	12	13	14	15	16	17
xx1	4.115	5.143	6.625	9.157	10.788	11.800	12.524	13.233	14.236	15.808
xx2	4.116	5.144	6.627	9.161	10.794	11.805	12.529	13.238	14.239	15.812
xx3	4.116	5.146	6.631	9.173	10.811	11.826	12.553	13.263	14.272	15.851
xx4	4.115	5.140	6.618	9.147	10.778	11.788	12.512	13.220	14.224	15.798
xx5	4.133	5.165	6.649	9.180	10.810	11.822	12.548	13.257	14.261	15.834
xx6	4.115	5.140	6.618	9.148	10.778	11.788	12.512	13.220	14.223	15.796
xx7	4.107	5.134	6.614	9.145	10.776	11.787	12.511	13.220	14.222	15.795
xx8	4.107	5.132	6.610	9.140	10.770	11.781	12.505	13.213	14.216	15.789
xx9	4.106	5.131	6.609	9.139	10.769	11.779	12.503	13.212	14.215	15.787
zx1	10.769	13.458	17.325	23.950	28.223	30.871	32.769	34.628	37.260	41.384
zx2	10.814	13.498	17.367	23.988	28.255	30.899	32.794	34.649	37.274	41.390
zx3	10.761	13.445	17.317	23.944	28.214	30.860	32.756	34.610	37.235	41.352
zx4	10.786	13.478	17.352	23.978	28.248	30.893	32.788	34.643	37.265	41.382
dx1	13.767	17.213	22.199	30.715	36.199	39.614	42.074	44.469	47.850	53.162
dx2	13.844	17.255	22.180	30.665	36.145	39.539	41.980	44.354	47.695	52.964
dx3	13.933	17.343	22.268	30.693	36.121	39.479	41.895	44.251	47.589	52.830
dx4	14.274	17.681	22.602	31.025	36.451	39.808	42.225	44.580	47.918	53.159
dx5	13.843	17.254	22.179	30.605	36.033	39.391	41.811	44.172	47.501	52.742
dx6	13.712	17.134	22.067	30.494	35.922	39.282	41.697	44.048	47.387	52.633
dx7	13.701	17.112	22.038	30.464	35.892	39.250	41.667	44.023	47.361	52.602
dx8	13.702	17.119	22.052	30.480	35.908	39.264	41.679	44.034	47.373	52.616
dx9	13.705	17.116	22.042	30.468	35.896	39.254	41.671	44.027	47.365	52.606
dx10	14.301	17.708	22.629	31.051	36.477	39.834	42.250	44.606	47.944	53.184

In the Dongsha fishery port, each boat is anchored by two anchors on the fore and aft. The forces of fore and aft are considered. By comparing the force exerted on the ship with the resultant force of the fore and aft (Table 11), it could be concluded that the resistance level of the Dongsha fishing against typhoon damage is 12.

Table 11. Force of anchor holding (kN).

Ship type	Force of anchor	Force of anchor chain	Resultant force	Resultant force of fore and aft
Small	5.145	4.704	9.849	12.804
Medium	17.15	4.704	21.854	28.410
Large	24.01	4.704	28.714	37.328

https://doi.org/10.5194/nhess-2021-82
Preprint. Discussion started: 29 March 2021

Natural Hazards and Earth System Sciences
Open Access
Discussions

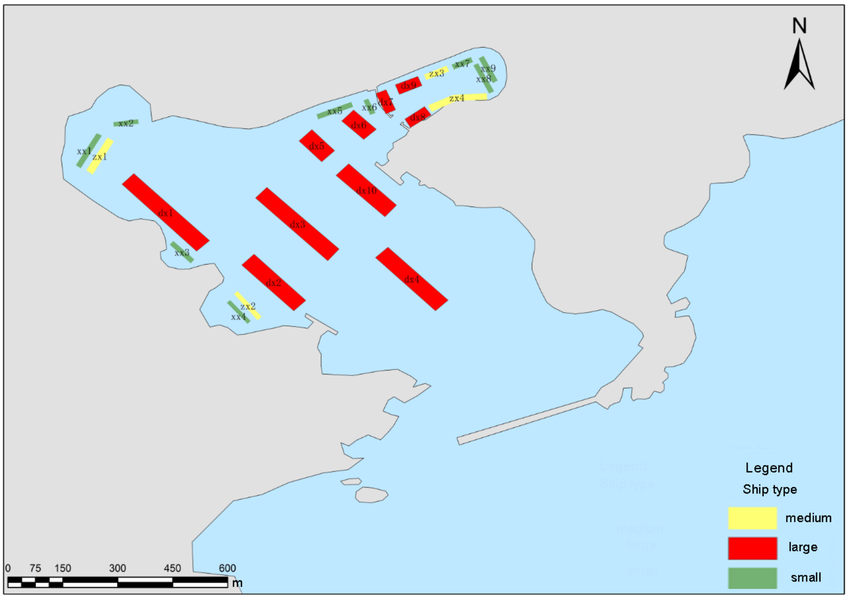

Figure 12. Feature points of the fishing boat anchoring water.

3.3 Shoreline

In consideration of the features of the Dongsha fishery port, 20 points were selected to represent the different types of shoreline (Fig. 13). Regarding the typhoon rating assessment for the shoreline, knowledge on the elevation of the coastline and the water was required. The water elevation was the height of the storm surge adding to 1/2 H_s. The results for the shoreline resilience to typhoons are shown in Table 12 and Fig. 13. The elevation of the shoreline should be higher than that of the water. Therefore, it could be concluded that the resistance level of Dongsha fishing against typhoon damage is 12.

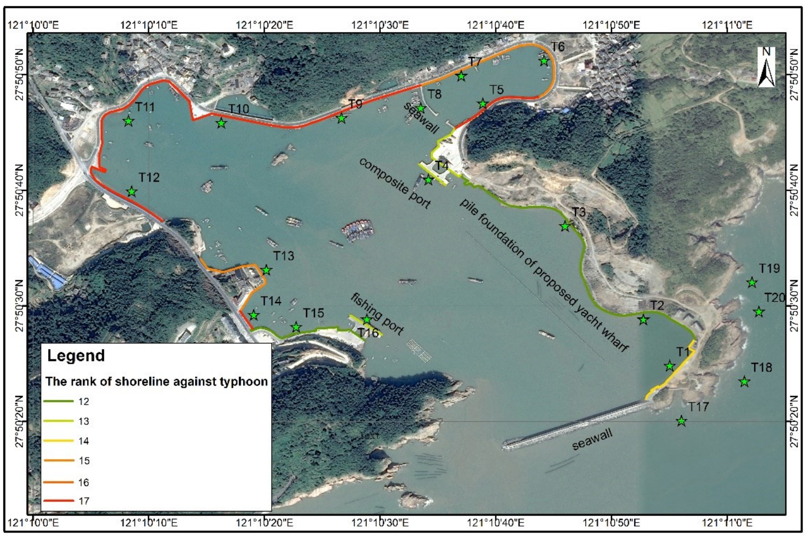

Figure 13. Feature points of different typhoon pathways scenarios (from © Google Earth).

Table 12. Water elevation and coastline elevation.

Point	Water elevation under different typhoon levels (m)	Coastline	Level

https://doi.org/10.5194/nhess-2021-82
Preprint. Discussion started: 29 March 2021

Natural Hazards and Earth System Sciences Discussions

	8	9	10	11	12	13	14	15	16	17	elevation (m)	result
T1	3.02	3.22	3.51	3.91	4.20	4.42	4.56	4.77	4.93	5.27	4.57	14
T2	3.05	3.26	3.56	3.98	4.27	4.51	4.67	4.87	5.02	5.37	4.43	12
T3	3.12	3.34	3.67	4.10	4.40	4.63	4.80	4.96	5.11	5.48	4.53	12
T4	3.10	3.30	3.59	4.00	4.29	4.50	4.65	4.81	4.96	5.26	4.53	13
T5	3.00	3.18	3.44	3.81	4.09	4.27	4.40	4.53	4.70	4.96	5.20	17
T6	2.99	3.17	3.43	3.79	4.06	4.24	4.37	4.50	4.67	4.92	4.52	15
T7	3.01	3.19	3.46	3.83	4.10	4.29	4.43	4.56	4.72	4.99	4.68	15
T8	3.03	3.23	3.50	3.89	4.16	4.36	4.50	4.63	4.79	5.06	4.17	12
T9	3.10	3.30	3.59	3.98	4.27	4.47	4.61	4.75	4.91	5.20	5.21	17
T10	3.07	3.27	3.55	3.95	4.24	4.44	4.59	4.72	4.88	5.17	5.27	17
T11	3.00	3.15	3.38	3.64	3.80	3.90	4.01	4.12	4.26	4.48	5.27	17
T12	3.04	3.24	3.51	3.84	4.07	4.23	4.31	4.43	4.59	4.84	5.56	17
T13	3.04	3.23	3.51	3.90	4.18	4.38	4.52	4.66	4.82	5.10	4.81	15
T14	3.01	3.21	3.48	3.87	4.15	4.34	4.48	4.62	4.77	5.05	5.36	17
T15	3.01	3.21	3.47	3.86	4.13	4.32	4.46	4.60	4.77	5.04	4.17	12
T16	3.05	3.24	3.53	3.92	4.20	4.41	4.56	4.71	4.87	5.15	4.56	13
T17	4.75	5.24	5.97	6.70	7.17	7.72	8.01	8.31	8.20	8.93	9.21	17
T18	4.77	5.25	5.95	6.72	7.19	7.78	8.10	8.38	8.25	8.89	12.23	17
T19	4.86	5.33	6.00	6.81	7.22	7.79	8.11	8.40	8.29	8.82	9.13	17
T20	4.83	5.31	5.98	6.77	7.20	7.79	8.10	8.38	8.26	8.80	9.13	17

3.4 Comprehensive assessment

According to the "Regulation for typhoon prevention assessment of fishery ports," there are two types of typhoon damage resistance levels for fishery ports. One represents the lowest level, while the other represents the comprehensive level. The lowest level of a fishery port represents the lowest values for the seawall, berth waters, and shoreline level, and the Dongsha fishery port was found to have a value of 12. The comprehensive level represents the weighted average of the seawall, berth waters, and shoreline level. The weighting factors of the seawall, berth waters, and shoreline are 0.25, 0.45, and 0.3, respectively. Hence, the calculated comprehensive level of the Dongsha fishery port is 12.

4 Discussion

The method introduced in this study is a practical technique for quantitatively assessing a fishery port's resilience to typhoon-related damage, and results are based on seawall, berth waters, and shoreline perspectives. Such an assessment of the resistance level of a fishery port against typhoon damage can reveal weaknesses in the port's defenses and allow for optimization of shelter spaces for fishing boats. The analysis carried out here had several caveats, which are important to highlight when considering these results. Notably, the level 12 for the Dongsha fishery port does not indicate that boats should be evacuated when a level 12 level typhoon is coming. However, when a level 12 typhoon slams into the Dongsha fishery port at the radius of maximum winds, boats should consider taking shelter. The feature points of T2, T3, T8, and T15 are the weaknesses of the Dongsha fishery port, and the port could enhance its defenses through increasing the elevation at these weakness points.

Considering the uniform standard, the analysis treated the distance from the fishery port to the storm track very roughly, which is the geometric mean radius of maximum wind. The other distance was also not taken into account in the assessment. In this analysis, all other impacts (sea level rise, rain, stability of infrastructure) were disregarded; the proposed methodology does not assess the total conditions of the fishery port.

https://doi.org/10.5194/nhess-2021-82
Preprint. Discussion started: 29 March 2021

Natural Hazards and Earth System Sciences
Open Access
EGU
Discussions

In addition to the assessment of the resilience of the fishery port to typhoons, the weather forecasting and warning systems established in Wenzhou have proven to be efficient at preventing human and economic losses from typhoons. Further, evacuation plans and disaster response and preparedness solutions should be employed.

5 Conclusion

Some of the damage to fishery ports from typhoons may be preventable. This study described a systematic and quantitative method for assessing the resilience of fishery ports to typhoons, and a case study was carried out on the Dongsha fishery port in Zhejiang Province, China. Historical typhoons were studied to identify the most useful typhoon pathways (south side toward the west) and scenarios (level 8–17 typhoons) for the assessment. The findings indicated that tide–surge interactions results, albeit these data were based on a limited number of events, are important to consider and the majority of the largest practical storm surges occurred around low tide; this was similar to the results in another study (Idier et al., 2012). Importantly, the Dongsha fishery port was found to have a resistance level of 12, and several points of weakness were identified where improvements in elevation could lessen impacts from future typhoons. In conclusion, the findings of this study demonstrated that this is a versatile framework for assessing fishing ports and developing disaster prevention plans. Though there remain a few constraints in its application (such as with regard to sea level rise, rain, and the stability of infrastructure), the proposed method should be readily applicable to other locations.

Author contribution Yachao Zhang and Jufei Qiu designed the versatile methodology for evaluation of the resilience of fishery ports to typhoons. Yachao Zhang and Xiaojie Zhang prepared the manuscript with contributions from all co-authors. Aifeng Tao, Jianli Zhao, Jianfeng Wang developed the model and performed the simulations. Yanfen Deng figures and Wentao Huang analysed the result.

Acknowledgments We are grateful to the Wenzhou Marine Environmental Monitoring Center and Dongtou Fishery Administration and Port Supervision station for providing basic data. This work was jointly supported by the Open Funds program of the Key Laboratory of Coastal Disaster and Defense, Ministry of Education (No. 201604), Key Laboratory of Integrated Marine Monitoring and Applied Technologies for Harmful Algal Blooms, S.O.A., MATHAB (No. MATHAB201804) and Youth Marine Science Foundation of East China Sea Bureau of Ministry of Natural Resources (No. 202002).

Declarations

Competing interests

Not applicable.

Availability of data

The datasets used during the current study are available from the corresponding author on reasonable request.

Code availability

Not applicable.

References

Abeshima, N., Amagai, K., Kimura, N., Nishimura, H.: Mooring limit of small fishing boat at kumaishi fishing port, J JPN INST NAV, 112(112): 345-352, http://dx.doi.org/10.9749/jin.112.345, 2017.

https://doi.org/10.5194/nhess-2021-82
Preprint. Discussion started: 29 March 2021

Natural Hazards and Earth System Sciences
Open Access
Discussions

Bertin, X., Bruneau, N., Breilh, J.F., Fortunato, A.B., Karpytchev, M.: Importance of wave age and resonance in storm surges: The case Xynthia, Bay of Biscay. OCEAN MODEL, 42(1):16-30, http://dx.doi.org/10.1016/j.ocemod.2011.11.001, 2012.

China Meteorological Administration GB/T 19201-2006 Grade of tropical cyclones, 2006.

Department of Natural Resources of Zhejiang Province: Bulletin of Zhejiang Marine Disaster, 2019.

DHI MIKE21 & MIKE 3 flow model FM hydrodynamic and transport module scientific documentation. Denmark, 2012.

Dongshui, C., Qionglin, F.: The typhoon risk assessment study of Xiamen fishery port based on the analytic hierarchy process. Qingdao Yuan Yang Chuan Yuan Zhi Ye Xue Bao 40(002): 54-58, cnki:sun:qdyy.0.2019-02-011, 2019.

Du, M., Hou. Y., Qi. P., Wang, K.: The impact of different historical typhoon tracks on storm surge: A case study of Zhejiang, China. J MARINE SYST, 103318, http://dx.doi.org/10.1016/j.jmarsys.2020.103318, 2020.

Flather, R. A.: Encyclopedia of ocean sciences || storm surges*. 530-540, 2001.

Fujita, T.: Pressure distribution within typhoon. GEOPHYS. Mag 23: 437-451, 1952.

Glahn, B., Taylor, A., Kurkowski, N.: Shaffer WA The role of the SLOSH model in national weather service storm surge forecasting. Natl Weather Digest, 33(1):3-14, 2009.

Huang, SJ.: Investigation on storm surge and erosion-deposition in Zhejiang coastal waters. Dissertation, Zhejiang University., 2017

Idier, D., Dumas, F., Muller, H.: Tide-surge interaction in the English Channel. NAT HAZARD EARTH SYS, 12(12):3709-3718, http://dx.doi.org/10.5194/nhess-12-3709-2012, 2012.

Kawaguchi, T., Hashimoto, O., Mizumoto, T., Kamata, A.: Construction of offshore fishing port for prevention of coastal erosion. American Society of Civil Engineers 24th International Conference on Coastal Engineering, Kobe, Japan http://dx.doi.org/10.1061/9780784400890.088, 1995.

Kong, XP.: A numerical study on the impact of tidal waves on the storm surge in the north of Liaodong Bay, ACTA OCEANOL SIN, 33 (1): 35-41, http://dx.doi.org/10.1007/s13131-014-0430-9, 2014.

Li, A., Guan, S., Mo, D., Liu, Z.: Modeling wave effects on storm surge from different typhoon intensities and sizes in the South China Sea, ESTUAR COAST SHELF S, 235, 106551, http://dx.doi.org/10.1016/j.ecss.2019.106551, 2019.

Ministry of Natural Resources of the People's Republic of China Bulletin of China Marine Disaster, 2019.

Ministry of Transport of the People's Republic of China JTS 144-1-2010 Load Code for Harbour Engineering, 2006.

NDRC, MARA , National plan for the construction of coastal fishery ports (2018-2025), 2018.

Prelligera, F. A., Caro, C. V., Ladiero, C., Alfredo, M. F. L., Lapidez, j. p., Malano, V., Agaton, r., and Santiago, J.: Storm Surge Modelling of Super Typhoon Haiyan Event in Tacloban City, Leyte using MIKE 21 Model, EGU General Assembly 2014, Vienna, Austria, 2014.

Premwadee, K., Phattrawan, T., Wanchamai K,: Trends in marine fish catches at pattani fishery port (1999-2003). Songklanakarin Journal of ence and Technology 28(4), 2006.

Shi, X. W., Han, Z. Q., Fang, J. Y., Guo, Z., Sun, Z.: Assessment and zonation of storm surge hazards in the coastal areas of China, NAT HAZARDS, 100(1): 39-48, 2020.

Shi, X. W., Qiu, J. F., Chen, B. R., Zhang, X., Bei, Z.: Storm surge risk assessment method for a coastal county in China: case study of Jinshan District, Shanghai, STOCH ENV RES RISK A, 34 (5): 627-640, 2020.

Sun, Z., Huang, S., Nie, H., Jiao, J., Huang, S., Zhu, L,. Xu, D.: Risk analysis of seawall overflowed by storm surge during super typhoon, OCEAN END, 107: 178-185, http://dx.doi.org/10.1016/j.oceaneng.2015.07.041, 2015.

Wang, J., Xu, S., Ye, M., Huang, J.: The mike model application to overtopping risk assessment of seawalls and levees in shanghai, INT J DISAST RISK SC, 2(4), 32-42, http://dx.doi.org/10.1007/s13753-011-0018-3, 2011.

Wang, X. N., Wang, X. W., Zhai J., Li, X., Huang, H., Li, C., Zheng, J., Sun, H.: Improvement to flooding risk assessment of storm surges by residual interpolation in the coastal areas of Guangdong Province, China. QUATERN INT, 453: 1-14, http://dx.doi.org/10.1016/j.quaint.2016.12.025, 2017.

https://doi.org/10.5194/nhess-2021-82
Preprint. Discussion started: 29 March 2021

Wang, Y. X., Gao, T., Jia, N., Han, Z. Y.: Numerical study of the impacts of typhoon parameters on the storm surge based on Hato storm over the pearl river mouth, china, REG STUD, 34, 101061, 2020.

Willoughby, H. E., Rahn, M. E.: Parametric Representation of the Primary Hurricane Vortex. Part I: Observations and Evaluation of the Holland (1980) Model, MON WEATHER REV, 134(12):1102-1120, http://dx.doi.org/10.1175/MWR2831.1, 2004.

Yang S, Li Y, Chen L (2017) The characteristics of tropical cyclone intensity change in western north pacific. Journal of Tropical Meteorology 33(5): 666-674.

Zhu, J. Z.,, Huang, G. X.: The prediction and visualization of a storm surge the Qiantang rive estuary, Zhejiang Hydrotechnics, 2002(03), 44-46, 2002.